Identifying a marked inflammation mediated cardiac dysfunction during the development of arthritis in collagen-induced arthritis mice

Z. Zhou[1], Z. Miao[2], A. Luo[3], D. Zhu[4], Y. Lu[2], P. Li[2], X. Feng[5], W. Tan[3], F. Wang[1]

[1]Department of Cardiology, [2]Department of Traditional Chinese Medicine; [3]Department of Rheumatology, the First Affiliated Hospital of Nanjing Medical University, Nanjing, China; [4]Department of Cardiology, Zhongda Hospital, Southeast University, Nanjing, China; [5]Integrated Traditional Chinese and Western Medicine Institute of Nanjing Medical University, Nanjing, China.

Abstract

Objective

Systemic inflammation is very closely linked to the increased risk of cardiovascular diseases (CVD) in rheumatoid arthritis (RA). We investigated the cardiac changes during the development of arthritis in collagen-induced arthritis (CIA) mice to explore the potential role of inflammation on cardiac dysfunction in RA.

Methods

Arthritis severity was evaluated using clinical indices, micro-computed tomography and histopathology. Cardiac function was determined by transthoracic echocardiography at weeks 5, 7, 9 and 11 after immunisation in mice. At week 7 (day 50), mice joints and hearts were removed for pathological study, and cardiomyocytes and cardiac fibroblasts were isolated using Langendorff perfusion method ex vivo to measure the expression of inflammatory and cardiac-related genes by real time PCR. The expression of key molecule in cardiac dysfunction (β-MHC) was also tested in H9c2 cardiomyocyte treated with sera derived from CIA mice or RA patients.

Results

At day 50 after immunisation, cardiac function in CIA mice was prominently reduced as evidenced by decreased ejection fraction (EF) and fractional shortening (FS), increased left ventricular end-systolic volume (LVESV) and internal systolic diameter (LVIDs). Accordingly, enhanced inflammatory cell infiltration and fibrosis were identified in ventricular tissues pathologically, and increased inflammatory gene expression including TNF-α, IL-6, IL-17 and MMP3 was detected in isolated ventricular cardiomyocytes and cardiac fibroblasts from CIA mice. Furthermore, H9c2 cells treated with sera from CIA mice or RA patients exhibited high levels of β-MHC.

Conclusion

Joint inflammation is associated with an obvious cardiac dysfunction and enhanced inflammation infiltration and inflammatory cytokine production in cardiomyocytes and cardiac fibroblasts during CIA development. Our data provide the direct evidence that inflammation contributes to the development of cardiac diseases in RA patients.

Key words

rheumatoid arthritis, inflammation, cardiac dysfunction, collagen-induced arthritis

*Zihao Zhou, MD**
*Zhengyue Miao, MD**
Aishu Luo, MD
Didi Zhu, PhD
Yan Lu, PhD
Peng Li, PhD
Xiaoke Feng, MD
Wenfeng Tan, PhD
Fang Wang, MD

**These authors contributed equally to this work.*

Please address correspondence to:
Fang Wang,
Department of Cardiology,
the First Affiliated Hospital of
Nanjing Medical University,
Nanjing 210029, China.
E-mail: wangfangheart@njmu.edu.cn

Wenfeng Tan,
Department of Rheumatology,
(address as above)
E-mail: tw2006@njmu.edu.cn

Received on December 19, 2018; accepted in revised form on April 29, 2019.

Funding: this project was sponsored by grants from the National Natural Science Foundation of China (no. 81671610, 81471610, 81471611, 81801625), and the Priority Academic Program Development of Jiangsu Higher Education Institutions (PAPD).

Competing interests: none declared.

Introduction

Rheumatoid arthritis (RA) is a systemic autoimmune disease that predominantly affects the peripheral joints and also involves multiple extra-articular organs (1). Ample evidence has indicated an increased risk of cardiovascular diseases (CVD) in patients with RA (2), and CVD has been a major cause of mortality in RA, accounting for about 39.6% of death in patients with RA, particularly due to coronary artery diseases, heart failure (3, 4). Increased cardiovascular risk in RA patients can not be fully explained by the traditional risk factors, such as hypertension, obesity, diabetes, age and smoking (5, 6). The underlying pathophysiological mechanism linking RA and cardiovascular diseases are far from being completely understood.

Recent evidence indicates a primary role of the chronic inflammation in RA contributing to the course of cardiac dysfunction. Increased C-reactive protein (CRP) and erythrocyte sedimentation rate (ESR), small and large joint swelling, rheumatoid nodules and vasculitis are independently associated with an increased risk of CVD-related death (4, 7). RA disease activity is not only predictive of cardiovascular events but also strongly correlates with cardiac function. Greater left ventricular strain and wall thickness were observed in RA patients than those in healthy controls and positively associated with RA diseases activity (8, 9). Indeed, histologic examination of coronary arteries and staining for citrullination in the myocardial interstitium of RA patients have revealed more evidence of inflammation linked to cardiac dysfunction (10). Notably, IL-1 blockade with anakinra showed the improvement of left ventricular contractility and relaxation in patients with RA (11, 12). Recent data suggest that TNF inhibition can reduce both RA disease activity and the risk of acute coronary syndrome, further strengthening the link of inflammation and CVD diseases in RA (13).

To better understand the RA-related inflammation driving CVD, many studies have begun to explore the cellular mechanisms. IL-33 expression in endothelial cells within aortic adventitia is correlated positively with the number of tender and swollen joints, suggesting a link between the systemic disease state and the local vascular tissue microlesion (14). Treating cultured vascular endothelial cells with sera from CIA mice or RA patients increased the expression of MCP-1-induced protein (MCPIP) but inhibited endothelial nitric oxide synthase phosphorylation, thereby leading to the endothelial dysfunction (15). Recently, Pironti and colleagues reported that collagen antibody-induced arthritis (CAIA) mice displayed oxidative stress and myocardial remodelling, which provides new evidence for inflammation in RA linked to impaired cardiac function (16).

Despite these intriguing findings, much more work is needed to elucidate the mechanism of chronic inflammation bridging RA and cardiovascular disease. In the past decades, most studies focused on clinical investigation finding the relationship between inflammation and CVD diseases in RA, perhaps the lack of an animal model to mimic both articular inflammation and cardiac dysfunction in RA hampers the research progress on molecular mechanism. Thus, we firstly examined whether the CIA mouse model – the most widely used model for RA – could mimic both articular inflammation and cardiac dysfunction in RA. We further investigated the pathological alternations of the heart during the development of arthritis in CIA mice. Our results show that inflammation during active RA has long-term consequences of cardiac dysfunction.

Materials and methods

Reagents

Bovine type II collagen was bought from Chondrex (Redmond, WA, USA). Complete Freund's adjuvant and incomplete Freund's adjuvant were from Sigma (St. Louis, MO, USA). PrimeScript®RT Master Mix was from TakaRa (Dalian, China) and SYBR Green PCR Master Mix was from Applied Biosystems (Carlsbad, CA, USA). Dulbecco's modified Eagle's medium (DMEM) and the other culture reagents from GIBCO (Carlsbad, CA, USA).

Induction of collagen-induced arthritis

Six-week-old male DBA/1J mice were

purchased from the Shanghai Laboratory Animal Center, Chinese Academy Sciences (Shanghai, China). The protocols for mouse feeding, sacrifice and tissue harvesting were approved by the Institutional Ethics Committee for Animal Experiments of Nanjing Medical University.

The mice were kept in a specific pathogen-free environment with standard mouse chow and water *ad libitum*. The arthritis was induced as described previously (17, 18). Briefly, the mice were injected intradermally into the base of the tail with 100 μl of an emulsion containing 100 μg of bovine type II collagen (CII) and complete Freund's adjuvant (CFA, containing 4 mg/mL *Mycobacterium tuberculosis*) as a primary immunisation. On day 21, mice were boosted with100μg of CII emulsified 1:1 with incomplete Freund's adjuvant (IFA). The same volume of normal saline was injected to the mice in the normal control group following the procedure above.

Severity assessment of arthritis

The mice were inspected daily for the food intake and onset of arthritis characterised by oedema and/or erythema in the paws up to 11 weeks after immunisation. A qualitative scoring system (arthritis index) was used to assess the occurrence and severity of arthritis in a blinded fashion as previously described (17). Briefly, each paw was evaluated and the arthritis index was scored individually on 0–4 scale according to the following criteria: 0 = no swelling; 1 = slight swelling and erythema confined to either ankle or mid foot; 2 = slight swelling extending from ankle to mid foot; 3 = moderate welling from ankle to metatarsal joints; 4 = severe swelling in the ankle, foot, and digits. Each paw was graded, and the severity score was the sum of the scores of each paw with the maximum score being 16.

Micro-computed tomography imaging analysis

Mice paws were removed at postmortem on day 50 and placed in 10% neutral buffered formalin for analysis of bone morphology by micro-computer tomography (micro-CT) following our published procedures (19). The samples were scanned using a micro-CT Sky-Scan1176 system with the following imaging parameters: spatial resolution of 9 μm, photo energy 50 kV and current of 500 μA, 0.5 mm aluminium filter, 180° scan, rotation step 0.7° and frame averaging of 1. For verification of bone destruction, 3-dimensional models of the knee joints and paws were reconstructed using SkyScan CT Analyzer v. 1.8 software (Bruker, Germany).

Cardiac imaging

Transthoracic echocardiography was performed at week 7 after immunisation in CIA mice and normal controls under light anaesthesia (50 mg/kg sodium pentobarbital, i.p.), with an ultrasound system (Vevo 2100, VisualSonics, Canada) using a 21-MHz probe to determine left ventricular function. The left ventricular end-diastolic volume (LVEDV), end-systolic volume (LVESV), internal systolic diameter (LVIDs), internal diastolic diameter (LVIDd), interventricular septal thickness in diastole (IVSd) and systole (IVSs) as well as the left ventricular posterior wall thickness in diastole (LVPWd) and systole (LVPWs) were measured. The left ventricular (LV) fractional shortening (FS), ejection fraction (EF), and LV mass were calculated as described previously (20). In another set, the echocardiography was performed at weeks 3, 5, 7, 9 and 11 after immunisation only in CIA mice following the above procedures. All measures were averaged over three consecutive cardiac cycles.

Joint histopathological analysis

The mice were euthanised on day 50, their ankles or paws were excised, fixed in 4% paraformaldehyde for 48 h, decalcified in 10% ethylene diamine tetraacetic acid (EDTA) solution for 3 weeks, embedded in paraffin and sectioned. The sections (4 μm) were stained with haematoxylin-eosin (HE) staining and studied the joint changes under the light microscope (Nikon FDX-35, Japan).

Heart tissue preparation and staining

Whole hearts of mice were perfused with cold phosphate buffered saline (PBS) and then left ventricular was isolated on day 50. One part of them was treated with Trizol reagent (Invitrogen) for further gene expression detection. The other part was fixed in 4% paraformaldehyde for 48 h, embedded in paraffin, and sectioned (4 μm). The sections were stained with HE and masson trichome by standard methods, and masson trichome stained areas were determined with Image-Pro Plus 6.3 software (Media Cybernetics). The sum of 5 fields per mouse (n=5 mice) was used for statistical analysis to determine significant difference.

Cell culture and treatment

Rat H9c2 cardiomyocytes were cultured in Dulbecco's modified Eagle's medium (DMEM) containing 10% fetal bovine serum (FBS), 100 U/mL penicillin and 100 U/mL streptomycin, in a humidified atmosphere of 5% CO_2 at 37ºC.

H9c2 cells were incubated with sera pooled from control or CIA mice (n=8) at the indicated concentrations for 24 h. In addition, H9c2 cells were also stimulated with sera from 5 healthy controls (HC) or 5 active RA patients respectively (defined as DAS28 scores >3.2 before the initiation of disease-modifying anti-rheumatic drug [DMARD] treatment). The diagnosis of RA fulfilled the American College of Rheumatology revised criteria for the diagnosis of RA (21). This study was approved by the Ethics Committee of the First Affiliated Hospital of Nanjing Medical University, and informed consent was obtained from all patients. Finally, after treatment, cells were collected for analysis of β-MHC expression by real time PCR.

Isolation mice cardiomyocytes and cardiac fibroblasts

Ventricular cardiomyocytes and fibroblasts were isolated from CIA and normal mice on day 50. After injection of heparin for 30 min, mice were anaesthetised and their hearts were rapidly excised and placed in cold Ca^{2+}-free Tyrode's solution (mmol/L: NaCl 130, KCl 5.4, $MgSO_4$ 1.2, NaH_2PO4 1.8, HEPES 5, taurine 20, 2, 3 BDM 10, glucose 10, PH 7.30). The ascending aortas were mounted onto a Langendorff

Table I. Primers used for quantitative real-time PCR.

Gene name	Forward (5' to 3')	Reverse (5' to 3')
Mouse TNF-α	AGGGATGAGAAGTTCCCAAATG	GGCTTGTCACTCGAATTTTGAGA
Mouse IL-1β	GCTTCCTGTGCAAGTGTCTGA	TCAAAAGGTGGCATTTCACAGT
Mouse IL-6	CTGCAAGAGACTTCCATCCAG	AGTGGTATAGACAGGTCTGTTGG
Mouse IL-17	CCTCACACGAGGCACAAGTG	CTCTCCCTGGACTCATGTTTGC
Mouse MMP1	CCTTGATGAGACGTGGACCAA	ATGTGGTGTTGTTGCACCTGT
Mouse MMP3	GGCCTGGAACAGTCTTGGC	TGTCCATCGTTCATCATCGTCA
Mouse MMP9	GCCTCAAGTGGGACCATCAT	CTCGCGGCAAGTCTTCAGA
Mouse ANP	GCTTCCAGGCCATATTGGAG	GGGGGCATGACCTCATCTT
Mouse BNP	GAGGTCACTCCTATCCTCTGG	GCCATTTCCTCCGACTTTTCTC
Mouse β-MHC	CATGGGATGGTAAGAAACGGG	TCCTCCAGTAAGTCGAAACGG
Mouse α-SMA	ATTGTGCTGGACTCTGGAGATGGT	TGATGTCACGGACAATCTCACGCT
Mouse TGF-β1	CCGAAGCGGACTACTATGCTAAA	GTTTTCTCATAGATGGCGTTGTTG
Mouse Col1a1	CAGGGTATTGCTGGACAACGTG	GGACCTTGTTTGCCAGGTTCA
Mouse Col3a1	TGGCACAGCAGTCCAACGTA	AAGGACAGATCCTGAGTCACAGACA
Mouse GAPDH	GCACAGTCAAGGCCGAG-AAT	GCCTTCTCCATGGTGGTGAA

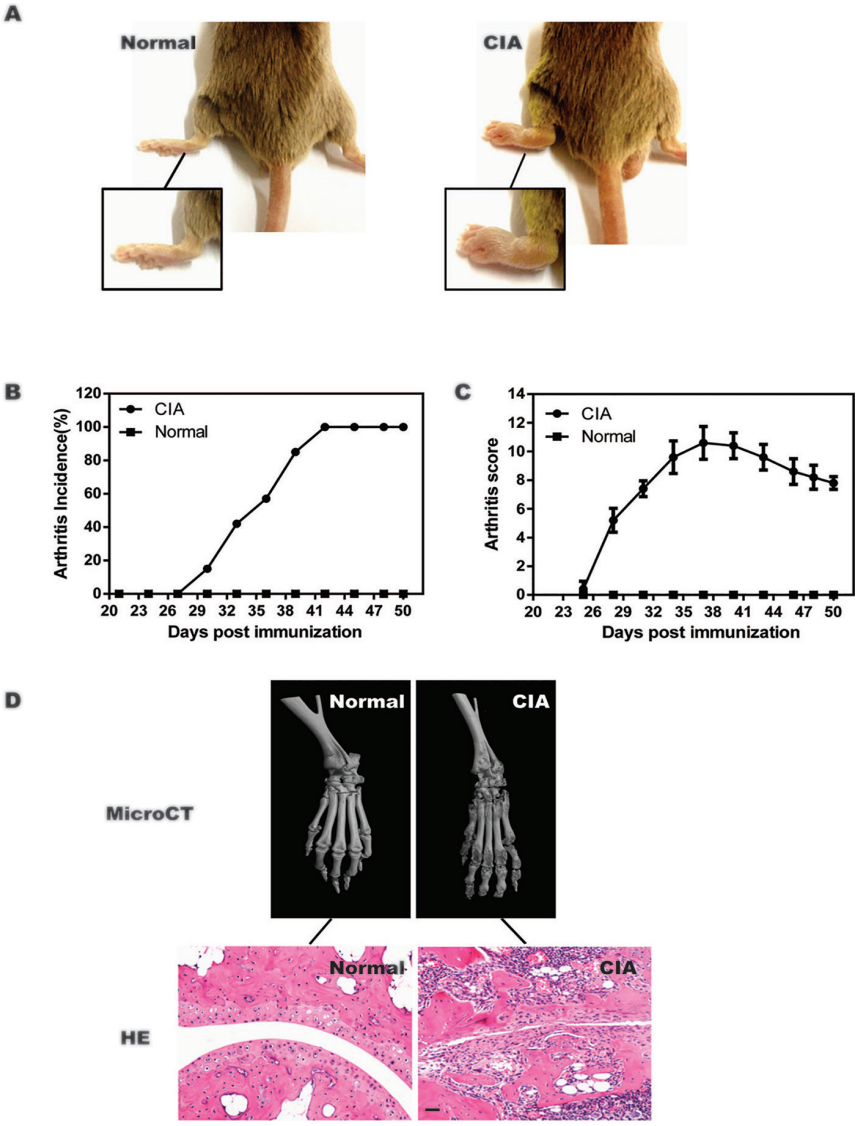

Fig. 1. Joint morphological and pathological changes in collagen-induced arthritis (CIA) mice. **A**: Swelling in multiple joints and palms of CIA mice; **B**: Arthritis incidence; **C**: Mean arthritis score (n=8, respectively); **D**: Representative micro-computed tomography (MicroCT) photographs (upper) and histological (bottom) features of increased synovial proliferation and inflammation in the joints of CIA mice. Scale bar: 50 μM.

perfusion system. The hearts was then perfused with Tyrode's solution for 2 min and Ca^{2+} free Tyrode's solution for 5 min, followed by 15 min-perfusion with the same buffer containing 0.5 mg/mL collagenase type II and 1% bovine serum albumin (BSA). When the hearts were soft and pale, they were removed to KB solution (mmol/L: L-glutamic acid 70, KCl 40, taurine 20, KH_2PO4 20, $MgCl_2$ 3, EGTA 0.5, glucose 10, KOH 50, sucrose 20, PH 7.40), the ventricles were cut into small pieces and dissected mechanically. The suspension was collected and centrifuged first at 50 g for 3 min to get cardiomyocytes; and then supernatant was centrifuged at 300 g for 5 min to obtain fibroblasts. Finally, all of the cells were treated with Trizol reagent for further gene expression detection.

Quantitative Real-Time Polymerase Chain Reaction (qRT-PCR)

Total RNA was extracted by use of Trizol reagent (Invitrogen) from mice LV tissue, H9c2 cells, isolated cardiomyocytes and fibroblasts. cDNA was synthesised using SYBR PrimeScript RT-PCR Kit according to the manufacturer's instructions. Gene expression levels of atrial natriuretic peptide (ANP), brain natriuretic peptide (BNP), α-smooth muscle actin (α-SMA), β-myosin heavy chain (β-MHC), collagen type I alpha 1 chain (Col1a1), collagen type III alpha 1 chain (Col3a1), transforming growth factor-β (TGF-β), IL-6, IL-1β, IL-17, TNF-α, matrix metallopeptidase 1(MMP1), MMP3 and MMP9 were evaluated by qRT-PCR on Applied Biosystems 7900HT Instrument (Applied Biosystems, CA, USA) following our established procedures (22). The primer sequences used in this study are summarised in Table I. Relative gene expression was determined by the $2^{-\Delta\Delta ct}$ method.

Statistical analysis

Statistical analyses were performed with SPSS software v. 18.0, and all figures were drawn using GraphPad Prism software v. 5.0. Data were expressed as the mean ± standard deviation (SD). Differences between two groups were performed with Student's *t*-test or a

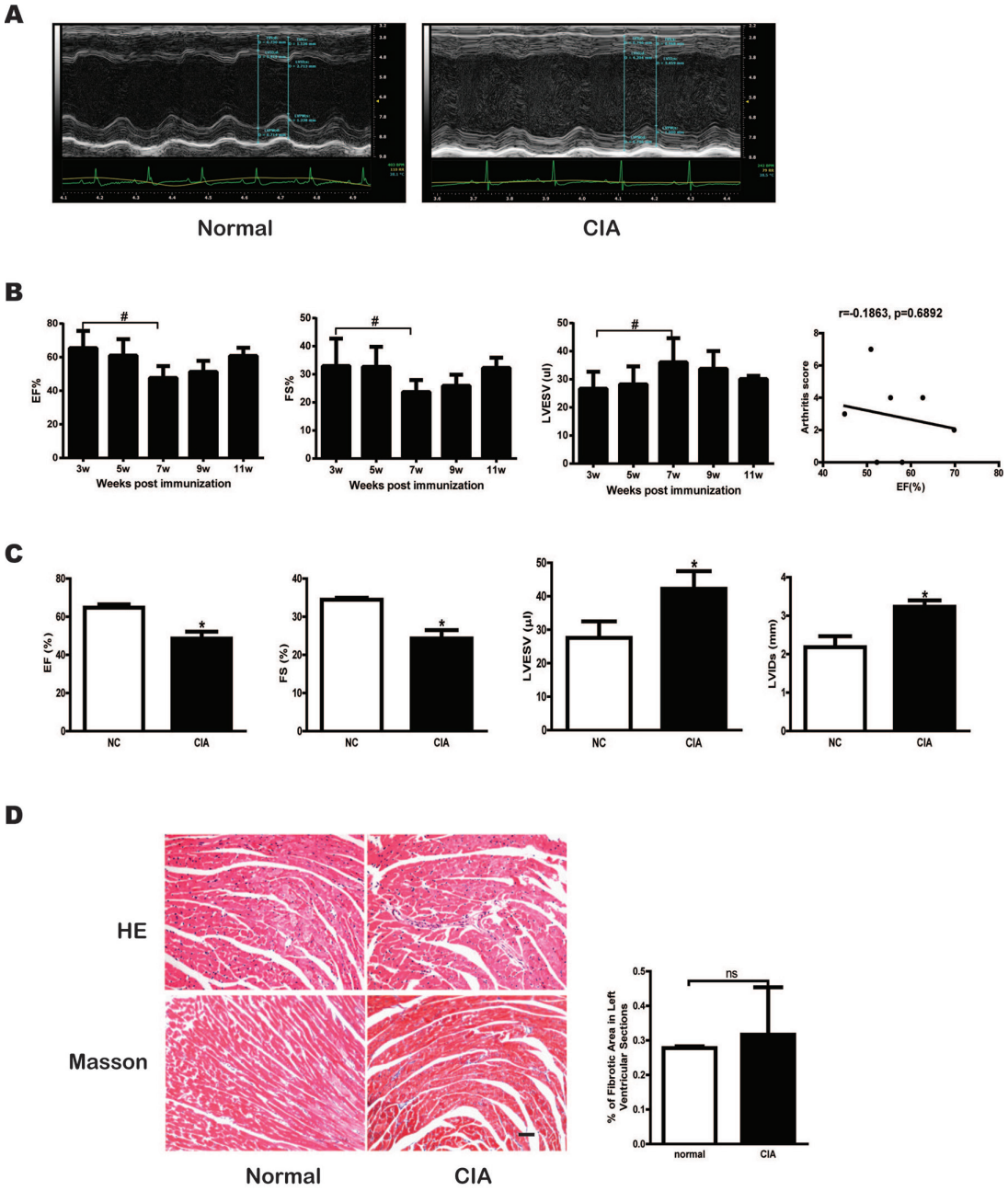

Fig. 2. Left ventricular (LV) functions were impaired in CIA mice.
A: Representative M-mode images of mice hearts at 7 week after immunisation. **B**: Quantification by echocardiography of ejection fraction (EF), fractional shortening (FS), and left ventricular end- systolic volume (LVESV) in mice at week 3, 5, 7, 9 and 11 week after immunisation. **C**: Quantification by echocardiography of EF, FS and left ventricular internal systolic diameter (LVIDs) in mice at 7 week after immunisation. (D) haematoxylin-eosin (HE) and masson trichrome staining for mice heart tissue at 7 week after immunisation. Scale bar: 50 μM. Values are expressed as mean ± SD from 8 mice per group. $^{\#}p<0.05$ compared with mice at 3 weeks after immunisation. $^{*}p<0.05$ compared with the normal control.

paired test for parametric data and Mann-Whitney *U*-test for non-parametric data. For all experiments, $p<0.05$ was taken as significant.

Results

Evaluation of collagen-induced arthritis

Paw swelling of mice was measured at day 21 and the measurement was continued until day 50. In collagen treated mice, arthritis appeared around day 25 post immunisation and severe paw redness and swelling were found about day 37 with the maximum of arthritis score 10.6±1.14 (Fig. 1A & C), and the arthritis incidence reached 100% on day 40 to 45 (Fig. 1B). On day 50, the animals were subjected to radiological and histopathological examinations. Representative radiographs of MicroCT revealed crude bone surface, bone erosion and narrowed joint space in the ankle joints of CIA mice, compared with normal controls (Fig. 1D, top). Consistently, HE staining showed that the CIA mice had a marked synovial proliferation, bone and cartilage inflammation and destruction (Fig. 1D, bottom).

Cardiac dysfunction in CIA mice

Because joint swollen began to attenuate at approximately week 6 after first immunisation, we sought to gain a better understanding of the cardiac function changes occurring during the course of arthritis. Accompanied joint swollen onset, EF%, FS% and LVESV in CIA mice were reduced to the lowest or highest level at about week 7 respectively, and all recovered to the normal level at week 11, which is in line with the time of joint swollen onset and arthritis remission in these CIA mice (Fig. 2A & B). Furthermore, we found arthritis score was inversely correlated with EF% in CIA mice, indirectly indicating arthritic inflammation contributing to cardiac dysfunction although without significant correlation (r=-0.1863, p=0.6892) (Fig. 2B).

In the other separate echocardiography examination, we next compared LV function and geometry changes in CIA mice at week 7 after immunisation with normal controls. CIA mice showed a significant decreased EF and FS levels but a clear increased LVESV and LVIDs as compared with the control mice (p<0.05) (Fig. 2C). LV mass, LVIDd, IVSd, IVSs, LVPWd and LVPWs did not significantly change in CIA mice (Table II). Histologically, HE staining was performed to check the inflammation and masson trichrome staining was used for detecting collagen deposition in LV tissue sections of mice at week 7 after immunisation. CIA mice showed significantly enhanced infiltration of inflammatory cells in heart tissue compared with normal controls (Fig. 2D). No significant fibrosis was observed in CIA and control mice.

Increased expression of proinflammatory and cardiac-related genes in left ventricular of CIA mice

To further confirm the contribution of inflammation to cardiac dysfunction, we examined mRNA levels of both proinflammatory (TNF-α, IL-1β, IL-6, MMP1, MMP3, MMP9) and cardiac function related genes (α-SMA, TGF-β1, ANP, BNP, β-MHC, Col1a1, Col3a1) in the whole LV tissues of mice. qRT-PCR analysis revealed that TNF-α, IL-6, MMP3, α-SMA, BNP, β-MHC, Col1a1, Col3a1mRNA levels were significantly enhanced in CIA mice at week 7 after immunisation compared with normal controls. IL-1β, MMP1, MMP9, TGF-β1 and ANP mRNA expression showed no significant changes although having increasing trend between the CIA and normal groups (Fig. 3).

Table II. Echocardiographic data of left ventricle in normal and CIA mice.

	Normal mice	CIA mice
n	10	10
EF (%)	64.79 ± 0.97	48.60 ± 2.12*
FS (%)	34.48 ± 0.29	24.32 ± 1.26*
LV mass (mg)	113.43 ± 6.56	112.07 ± 0.18
LVEDV (ul)	77.93 ± 5.88	81.88 ± 2.57
LVESV (ul)	27.61 ± 2.83	42.25 ± 3.06*
LVIDd (mm)	4.18 ± 0.13	4.27 ± 0.06
LVIDs (mm)	2.71 ± 0.11	3.23 ± 0.10*
IVSd (mm)	0.72 ± 0.02	0.69 ± 0.01
IVSs (mm)	1.23 ± 0.03	1.11 ± 0.02
LVPWd (mm)	0.75 ± 0.02	0.73 ± 0.01
LVPWs (mm)	1.31 ± 0.04	1.13 ± 0.03

Values are expressed as mean ± SD. *p<0.05 compared with the control.
EF: ejection fraction; FS: fractional shortening; LV: left ventricular; LVEDV: left ventricular end-diastolic volume; LVESV: left ventricular end-systolic volume; LVIDd: left ventricular internal diastolic diameter; LVIDs: left ventricular internal systolic diameter; IVSd: interventricular septal thickness in diastole; IVSs: interventricular septal thickness in systole; LVPWd: left ventricular posterior wall thickness in diastole; LVPWs: left ventricular posterior wall thickness in systole.

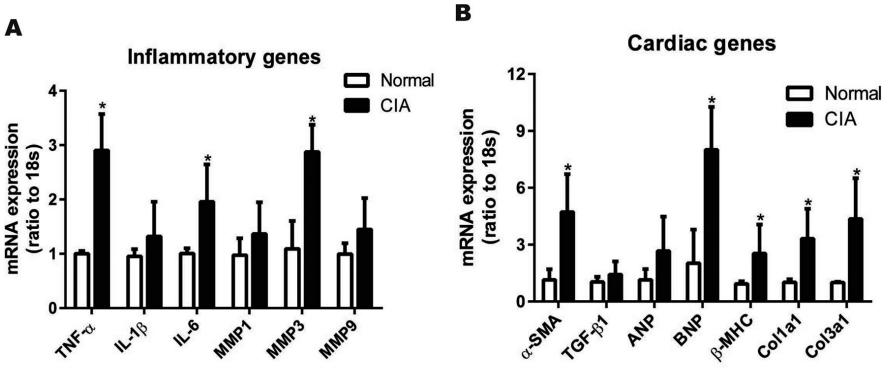

Fig. 3. Increased expression of genes related to inflammation and cardiac dysfunction in CIA mice heart.
A: Proinflammatory genes mRNA levels for TNF-α, IL-1β, IL-6, MMP1, MMP3, MMP9; **B**: genes related to cardiac dysfunction α-SMA, TGF-β1, ANP, BNP, β-MHC, Col1a1 and Col3a1 in hearts of mice at week 7 after immunisation were determined by quantitative real-time PCR. Relative gene expression was determined by the $2^{-\Delta\Delta ct}$ method. Values are expressed as mean ± SD from 8 mice per group.
*p<0.05 compared with the normal control.

Increased expression of proinflammatory and cardiac genes in cardiomyocytes and cardiac fibroblasts in CIA mice

Considering that both cardiomyocytes and cardiac fibroblasts are the most abundant cells in the cardiac tissues, we sought to investigate which cells are mostly affected by inflammation. Ventricular cardiomyocytes and cardiac fibroblasts were isolated from the mice at week 7 after immunisation and controls using Langendorff perfusion system *ex vivo*. Then cells were collected and assessed by qRT-PCR. As to inflammatory genes expression level, TNF-α was predominantly increased in cardiomyocytes and IL-17 was elevated in cardiac fibroblasts from CIA mice compared to normal controls. And cardiac genes showed no significant changes in either cardiomyocytes or cardiac fibroblasts in mice (Fig. 4). These data indicate that arthritis inflammation is linked to enhanced cardiac inflammation level in cardiomyocytes and fibroblasts.

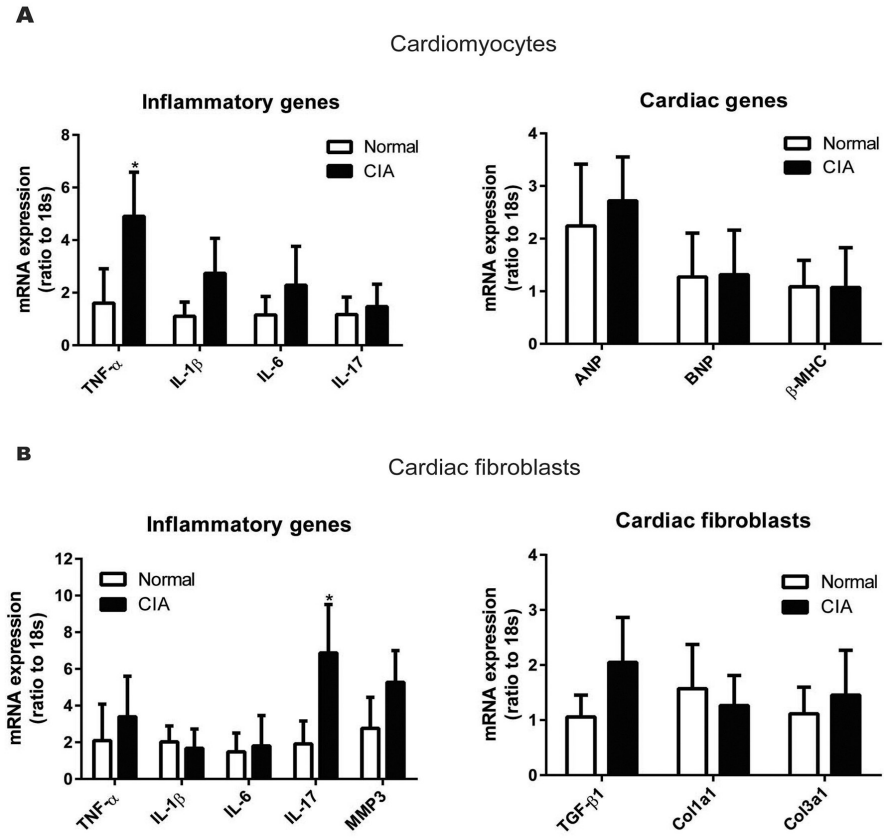

Fig. 4. mRNA expression of proinflammatory and cardiac genes in isolated cardiomyoctes and fibroblasts from mice heart.
A: mRNA expression of TNF-α, IL-1β, IL-6, IL-17, ANP, BNP, β-MHC in isolated cardiomyocytes; **B**: TNF-α, IL-1β, IL-6, IL-17, MMP3, TGF-β1,Col1a1 and Col3a1 in isolated cardiac fibroblasts from hearts of mice at week 7 after immunisation were determined by qPCR. Relative gene expression was determined by the $2^{-\Delta\Delta ct}$ method. Values are expressed as mean ± SD from 8 mice per group.
*p<0.05 compared with the normal control.

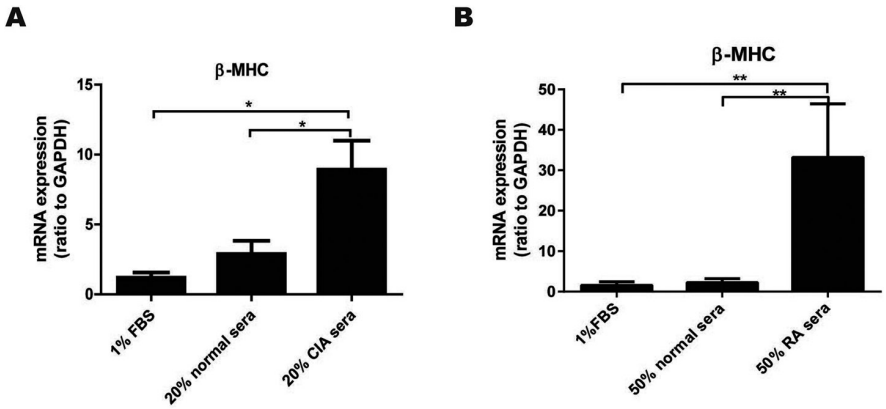

Fig. 5. Increased β-MHC mRNA level in H9c2 cells after treatment with sera from CIA mice or patients with RA.
A: H9c2 cells were incubated with sera pooled from control or CIA mice (n=8), or **B** sera from healthy controls or patients with RA (n=5) at the indicated concentration for 24 h. β-MHC mRNA was determinate by qPCR method. Values are expressed as mean ± SD from 3 independent experiments.
*p<0.05, **p<0.01 as compared with the respective control group.

Inflammation promoted mRNA levels of β-MHC in rat cardiomyocytes

To examine whether CIA-associated inflammation affected cardiomyocytes function directly, we incubated rat cardiomyocytes H9c2 with sera pooled from CIA or normal mice for 48 h *in vitro*, respectively. β-MHC expression was markedly induced by 3.08 and 7.48-fold in cells treated with CIA sera as compared with FBS or normal sera treated groups respectively (Fig. 5A). Similar results were obtained with H9c2 cells treated with sera from RA patients (Fig. 5B). In line with the results in Figure 5A, β-MHC mRNA level was significantly increased by 15.32 and 22.04 fold in H9c2 cells treated with RA patient sera when compared to the other two groups respectively. These data suggest that systematic inflammation could directly resulted in dysregulated function in cardiomyocytes in RA patients.

Discussion

We recently showed that levels of large artery compliance (C1) and small artery compliance (C2) were significantly decreased in RA patients compared with healthy controls, and the levels of ESR was correlated with the abnormal large artery compliance (23). Recently Pironti *et al*. report CAIA mice have impaired myocardial contractility *in vivo* and impaired calcium handling *in vitro* in the *'late phase'* of arthritis (16), which further provides molecular evidences for pathological changes occurring in the heart during RA disease. Despite these first exciting observations, how an articular or systemic inflammation leads to direct cardiac dysfunction remains largely unexplored during the pathogenesis of RA.

To address this issue, we first examined the relationship between arthritis progress and changes of cardiac function consecutively at different time after immunisation in CIA mice. In CIA mice, the maximum of arthritis score appeared at around week 5 and last about 1 week, and then began to attenuate. Interestingly, as evidenced by transthoracic echocardiography, significant reduction of left ventricular EF%, FS% as well as increased LVESV was found not at the peak of inflammation (at 5–6 weeks after immunisation) but the remission state (at 7–9 weeks after immunisation) in CIA mice. Further analysis showed that arthritis score was inversely correlated with EF% in CIA mice although without statistic difference, and heart weight–body weight ratio was not

changed either (data not shown). These data appears to show cardiac impairment present obviously in the remission of arthritis activity, supporting the idea that controlling joint or systematic inflammation is especially important for reduction cardiac events onset in RA (24). To further confirm the time course of inflammation and cardiac dysfunction, we used transthoracic echocardiography again to compare cardiac function in CIA mice at week 7 after immunisation with normal controls. In accordance with the above results, 25% and 29% decrease of EF% and FS%, 53% and 49% increase in LVESV and LVID respectively were found in CIA mice at week 7 after immunisation compared to normal controls, although the impairment was slighter in magnitude than typically seen in mice with overt cardiac injury, such as myocardial infarction and heart failure. We next explored whether inflammation was able to affect the pathological change of heart from CIA mice at week 7 after immunisation. Histologically, the hearts from CIA mice displayed much more inflammatory cells infiltration and higher degree of fibrosis, whereas, no significant difference in fibrosis area was observed. Together, our data from echocardiography and histology indicate that hearts from the arthritis model mice display impaired and morphological change in the remission phase of arthritis, which is about 2 weeks later than the time at the peak arthritis phase, though the overt signs of arthritis were gone, and the findings resemble medically controlled RA or RA in remission. Thus, in the following experiments, CIA mice at week 7 after immunisation were chosen as the experimental subjects. These observations were consistent with the results from CAIA mice where cardiac impairment was also detected in the post inflammatory phase although with different days of arthritis onset (57–89 days after arthritogenic antibody induction) due to different arthritis mouse models (16). To be different, cardiac fibrosis was not found in our study but significantly increased in CAIA mice as previously demonstrated by Pironti *et al*. (16), maybe due to stronger arthritic activity in CAIA mice than CIA mice.

Next, at the molecular level, mRNA levels of inflammatory and cardiac-related genes were examined in the whole heart and isolated cardiomyocytes or cardiac fibroblasts from hearts of CIA mice and normal controls. The expression of genes involved in inflammation (TNF-α, IL-6, MMP3) and cardiac function (α-SMA, BNP, β-MHC, Col1a1 and Col3a1) was significantly increased in the whole heart tissues of CIA mice, in addition, proinflammatory cytokines TNF-α and IL-17 are significantly induced in isolated cardiomyocytes or cardiac fibroblasts respectively from hearts of CIA mice, whereas no clear change of genes related to cardiac function were observed in neither isolated cardiomyocytes nor cardiac fibroblasts. TNF-α is believed to be critical for RA, and has also been proposed to lead to direct cardiomyocyte dysfunction and injury (25). In line with the finding in CAIA mice (16), we found that in CIA mice the whole hearts, isolated cardiomyocytes and cardiac fibroblasts displayed increased gene expression of TNF-α, highlighting TNF-α locally in the heart that may act as a local driver of cardiac injury. It has been reported that IL-17 accelerates myocardial fibrosis in animal models of heart injury *in vivo* (26), and *in vitro* the addition of IL-17 and TNF-α to endothelial cells induced a pro-inflammatory, pro-thrombotic, and pro-coagulant state (27). We detected higher mRNA expression of IL-17 in isolated cardiac fibroblasts from CIA mice than controls. Cardiomyocytes and cardiac fibroblasts accounts for about 90% of the cell populations of the whole heart (28), of which activated cardiomyocytes can produce and secrete a wide range of inflammatory and pro-fibrotic mediators, and cardiac fibroblasts are the main effector cells in cardiac fibrosis, meanwhile cardiac fibroblasts also impact myocardial development and remodelling through intercellular contact with cardiomyocytes. Although we did not observe significant changes of genes expression related to cardiac genes in isolated cardiac fibroblasts, we can not rule out the possibility that proinflammatory cytokines produced in cardiomyocytes may promote profibrogenic signalling in cardiac fibroblasts.

As proved in our present data in concordant with previous literature strongly showing persistent expression of proinflammatory cytokines locally in the heart may more specifically target cardiomyocytes thus to cause pathological changes of the heart (16, 20). Whether a systemic inflammation is responsible for arthritis and cardiomyocytes dysfunction remains unknown. We further compared the levels of β-MHC, which is commonly used to detect cardiac remodelling and hypertrophy, in rat cardiomyocytes H9c2 treated with sera from CIA or RA patients *in vitro*. Sera from CIA and RA patients strongly induced the expression of β-MHC in H9c2 cells, which provides the direct evidence that circle cytokines released during RA chronic inflammation may play an important role in mediating RA-related cardiac dysfunction.

Overall, the current study shows direct evidences that RA-related articular or systemic inflammation could impair cardiac function during the pathogenesis of RA disease. Although the cardiac function might be recovered owing to the signs of arthritic inflammation subside in CIA mice, the persistent joint and systemic inflammation in RA patients may induce severe heart injury as shown in typical impaired cardiac dysfunction. Thus, early management of inflammation is essential to reduce the burden of cardiovascular diseases among patients with RA. Despite these intriguing findings, much more work is needed to elucidate the proinflammatory networks bridging RA and cardiovascular disease.

Conclusions

In conclusion, our study provides cellular and molecular evidences supporting the hypothesis that RA-related inflammation plays a role in triggering cardiovascular risk, and highlights the inflammation as a potential preventive and therapeutic target for CVD in patients with RA.

References

1. CALABRESI E, PETRELLI F, BONIFACIO AF, PUXEDDU I, ALUNNO A: One year in review 2018: pathogenesis of rheumatoid arthritis. *Clin Exp Rheumatol* 2018; 36: 175-84.
2. SOLOMON DH, GOODSON NJ, KATZ JN *et al*.:

Patterns of cardiovascular risk in rheumatoid arthritis. *Ann Rheum Dis* 2006; 65: 1608-12.
3. SOKKA T, ABELSON B, PINCUS T: Mortality in rheumatoid arthritis: 2008 update. *Clin Exp Rheumatol* 2008; 26: S35-61.
4. ENGLAND BR, THIELE GM, ANDERSON DR, MIKULS TR: Increased cardiovascular risk in rheumatoid arthritis: Mechanisms and implications. *Bmj* 2018; 361: k1036.
5. JAFRI K, BARTELS CM, SHIN D, GELFAND JM, OGDIE A: Incidence and management of cardiovascular risk factors in psoriatic arthritis and rheumatoid arthritis: A population-based study. *Arthritis Care Res* (Hoboken) 2017; 69: 51-7.
6. AN J, ALEMAO E, REYNOLDS K *et al*.: Cardiovascular outcomes associated with lowering low-density lipoprotein cholesterol in rheumatoid arthritis and matched nonrheumatoid arthritis. *J Rheumatol* 2016; 43: 1989-96.
7. KAPLAN MJ: Cardiovascular complications of rheumatoid arthritis: Assessment, prevention, and treatment. *Rheum Dis Clin North Am* 2010; 36: 405-26.
8. FINE NM, CROWSON CS, LIN G, OH JK, VILLARRAGA HR, GABRIEL SE: Evaluation of myocardial function in patients with rheumatoid arthritis using strain imaging by speckle-tracking echocardiography. *Ann Rheum Dis* 2014; 73: 1833-9.
9. MIDTBO H, GERDTS E, KVIEN TK *et al*.: Disease activity and left ventricular structure in patients with rheumatoid arthritis. *Rheumatology* (Oxford) 2015; 54: 511-9.
10. AUBRY MC, MARADIT-KREMERS H, REINALDA MS, CROWSON CS, EDWARDS WD, GABRIEL SE: Differences in atherosclerotic coronary heart disease between subjects with and without rheumatoid arthritis. *J Rheumatol* 2007; 34: 937-42.
11. DEL BUONO M, ABBATE A, TOLDO S: Interplay of inflammation, oxidative stress and cardiovascular disease in rheumatoid arthritis. *Heart* 2018; 104: 1991-2.
12. IKONOMIDIS I, LEKAKIS JP, NIKOLAOU M *et al*.: Inhibition of interleukin-1 by anakinra improves vascular and left ventricular function in patients with rheumatoid arthritis. *Circulation* 2008; 117: 2662-9.
13. POPE JE: Rheumatoid arthritis: TNF inhibitors and cardiovascular risk management in ra. *Nat Rev Rheumatol* 2016; 12: 317-8.
14. AHMED A, HOLLAN I, CURRAN SA *et al*.: Brief report: Proatherogenic cytokine microenvironment in the aortic adventitia of patients with rheumatoid arthritis. *Arthritis Rheumatol* 2016; 68: 1361-6.
15. HE M, LIANG X, HE L *et al*.: Endothelial dysfunction in rheumatoid arthritis: The role of monocyte chemotactic protein-1-induced protein. *Arterioscler Thromb Vasc Biol* 2013; 33: 1384-91.
16. PIRONTI G, BERSELLINI-FARINOTTI A, AGALAVE NM *et al*.: Cardiomyopathy, oxidative stress and impaired contractility in a rheumatoid arthritis mouse model. *Heart* 2018; 104: 2026-34.
17. BRAND DD, LATHAM KA, ROSLONIEC EF: Collagen-induced arthritis. *Nat Protoc* 2007; 2: 1269-75.
18. GAN K, XU L, FENG X *et al*.: Celastrol attenuates bone erosion in collagen-induced arthritis mice and inhibits osteoclast differentiation and function in rankl-induced raw264.7. *Int Immunopharmacol* 2015; 24: 239-46.
19. FENG X, SHI Y, XU L, PENG Q *et al*.: Modulation of il-6 induced rankl expression in arthritic synovium by a transcription factor sox5. *Sci Rep* 2016; 6: 32001.
20. VERMA SK, KRISHNAMURTHY P, BAREFIELD D *et al*.: Interleukin-10 treatment attenuates pressure overload-induced hypertrophic remodeling and improves heart function via signal transducers and activators of transcription 3-dependent inhibition of nuclear factor-kappab. *Circulation* 2012; 126: 418-29.
21. LU LJ, BAO CD, DAI M *et al*.: Multicenter, randomized, double-blind, controlled trial of treatment of active rheumatoid arthritis with t-614 compared with methotrexate. *Arthritis Rheum* 2009; 61: 979-87.
22. XU L, PENG Q, XUAN W *et al*.: Interleukin-29 enhances synovial inflammation and cartilage degradation in osteoarthritis. *Mediators Inflamm* 2016; 2016: 9631510.
23. WANG L, TAN W, WANG F *et al*.: Artery compliance in patients with rheumatoid arthritis: Results from a case-control study. *Clin Rheumatol* 2018; 37: 169-77.
24. PRASAD M, HERMANN J, GABRIEL SE *et al*.: Cardiorheumatology: Cardiac involvement in systemic rheumatic disease. *Nat Rev Cardiol* 2015; 12: 168-76.
25. GRUNDTMAN C, HOLLAN I, FORRE OT, SAATVEDT K, MIKKELSEN K, LUNDBERG IE: Cardiovascular disease in patients with inflammatory rheumatic disease is associated with up-regulation of markers of inflammation in cardiac microvessels and cardiomyocytes. *Arthritis Rheum* 2010; 62: 667-73.
26. FENG W, LI W, LIU W, WANG F, LI Y, YAN W: IL-17 induces myocardial fibrosis and enhances rankl/opg and mmp/timp signaling in isoproterenol-induced heart failure. *Exp Mol Pathol* 2009; 87: 212-8.
27. HOT A, LENIEF V, MIOSSEC P: Combination of IL-17 and TNFalpha induces a pro-inflammatory, pro-coagulant and pro-thrombotic phenotype in human endothelial cells. *Ann Rheum Dis* 2012; 71: 768-76.
28. VLIEGEN HW, VAN DER LAARSE A, CORNELISSE CJ, EULDERINK F: Myocardial changes in pressure overload-induced left ventricular hypertrophy. A study on tissue composition, polyploidization and multinucleation. *Eur Heart J* 1991; 12: 488-94.